Proceedings of the 3rd ICMEM
International Conference on Mechanical Engineering and Mechanics
October 21–23, 2009, Beijing, P. R. China

# An interpretative model of g-g diagrams of racing motorcycle

Francesco Biral [1], Roberto Lot[2]

[1]DIMS-Dep. of Mechanical and Structural Engineering, University of Trento, Via Mesiano, 77, 38050 Trento, Italy
[2]DIMEG-Dep. of Innovation in Mechanics and Management, University of Padova, Via Venezia, 1, 35131 Padova, ITALY

**Abstract:** In this paper an analytical interpretative model is used to explain some peculiar features of normalized accelerations diagrams (g-g diagrams) of racing motorcycles. The shape of this diagrams has the twofold meaning of quantify the motorcycle maneuverability and evaluate the rider's maneuver performance. Experimental evidence shows that the envelope of the g-g diagram produced by racing motorcycle riders do not completely fill the ellipse of adherence. Specifically the combined braking and cornering maneuver is the most critical for a racing rider and only the best ones can reach the limits of the ellipse of adherence in such conditions. To interpret and understand this behavior, the theoretical g-g diagrams are analytically derived that are comparable with the experimental ones. The analytic approach is used to explain the shape of the acceleration envelop both for combined cornering-braking maneuvers and cornering-traction maneuvers. Finally, the optimal braking maneuver is calculated to prove that a correct driving strategy will completely fill the ellipse of adherence. However, the latter is not always physically possible since also the motorcycle design parameters affects the envelope of accelerations. Therefore, the influence of the centre of mass position on the g-g diagrams is analyzed and discussed and it is shown that a proper design can improve the motorcycle performance.

**Keywords: racing motorcycle, rider performance, theoretical model, g-g diagrams, optimal braking**

## 1 Introduction

The g-g diagrams are very popular tools to characterize the racing driver's capabilities to push the vehicle to its physical limits [1-4]. The g-g diagrams' basic concept is to plot longitudinal versus lateral accelerations of a vehicle, scaled with respect to gravity. It is a general property that the envelope of the maximum lateral and longitudinal accelerations is a sort of ellipse/circle (known as ellipse of adherence). It is well know that the reason of this shape is due to the tire behavior when combined longitudinal and lateral forces are present at the same time and the maximum values represent the tire lateral and longitudinal adherence or grip coefficients. With respect to adherence limits, the influence of suspensions and other vehicle subsystems on the g-g shape is minor, since they only make it easier or more difficult to the driver to reach those limits. In other words they affect the vehicle handling, while the envelope of g-g diagrams defines the maneuverability of the vehicle (the set of admissible motions) [5]. It is the racing driver skill or the presence of automatic subsystems, backed up by the vehicle handling characteristics, which makes it possible to completely fill the accelerations envelope. For this reasons the g-g diagrams are used to compare drivers' abilities or refine them for a particular vehicle. Although, it is widely used in the automotive field, not much is found in the literature concerning motorcycle. In particular experimental g-g diagrams produced by MotoGP racing riders show the peculiar characteristics that the acceleration envelopes do not completely fill the ellipse of adherence both in braking and traction conditions. The focus of this work is the interpretation of the above experimental g-g diagrams with the aid of an analytical model. A theoretical explanation of the special envelope shape is given and the influence of main motorcycle design parameters is analyzed. Finally, the theoretical optimal braking maneuver is found to prove that a correct driving strategy will completely fill the ellipse of adherence when physically possible.

## 2 Experimental g-g diagrams produced by motorcycle racing raiders

Figure 1 shows some experimental g-g diagrams of different motorcycles for two circuits. It is quite evident that, for all of them, the normalized acceleration envelop is different than the estimated ellipse of adherence (ellipse with dash line).

Figure 1 (a) and (b) show the g-g diagrams of a 125cc MotoGP machine respectively for Le Mans and Mugello circuits. Higher lateral accelerations and asymmetry in the circuit of Mugello are due to road bank in some corners. The pattern of accelerations in traction area are bounded by the engine power limit (which is relatively low for 125cc motorcycles). On the contrary during hard braking a sort of triangular shape for the deceleration envelope is produced. This is more evident for the SBK motorcycle (see Figure 1 (c)), which also yields a different envelop shape in the maximum traction area. For high power motorcycles the engine power is not the limiting factor and the load transfer take the scene as may restraining factor. The overall picture of the acceleration pattern looks like more to a "heart" shape than an ellipse. What is the reasons of this behaviour? Has it any influence on the lap time performance? An answer to these questions will be given in the following sections with the aid of a theoretical model.

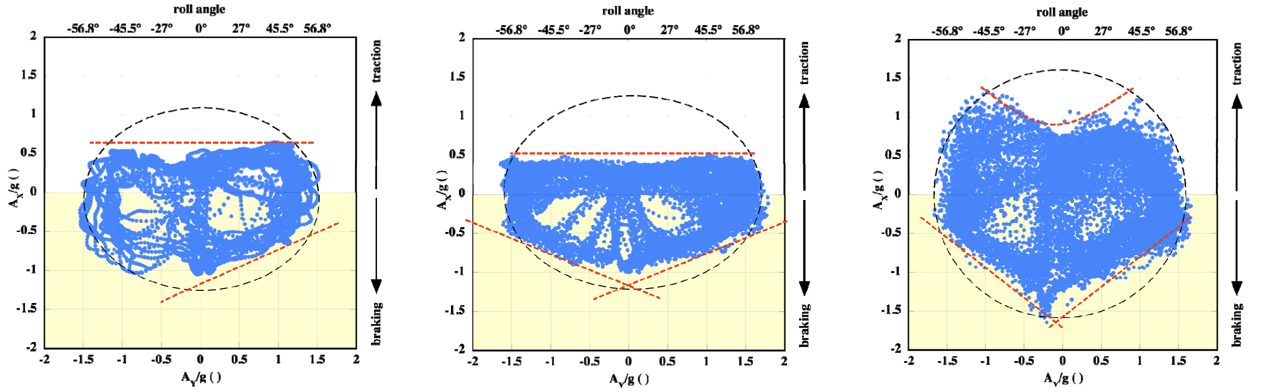


(a) 125cc MotoGP bike at Le Mans circuit

(b) 125cc MotoGP bike at Mugello circuit

(c) Superbike motorcycle at Mugello circuit

Figure 1 G-G diagram for different motorcycles in different circuits.

## 3 Interpretative model

### 3.1 Model description and equation of motions

In order to interpret the experimental data, a simplified dynamic model of the rider-motorcycle system is derived. The adopted model considers the rider-motorcycle system as a single rigid body, therefore the suspension motion is neglected. Moreover, the yaw motion is considered dependent of the lateral acceleration and forward speed (i.e. lateral speed is neglected). Aerodynamic drag force is at first neglected and its influence discussed later on in the article. Longitudinal, lateral and vertical forces are considered at the rear and front contact points. The so far described model has three degrees of freedom: longitudinal and lateral translational motion and roll rotation described in SAE coordinate system (see Figure 2).

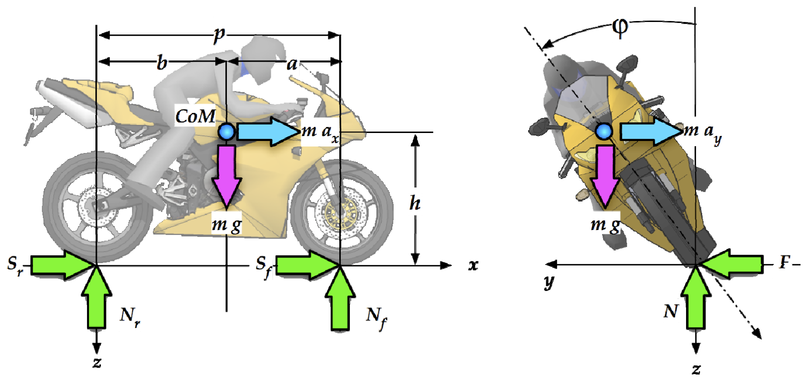


Figure 2 – Rigid-body motorcycle model. Forward acceleration and centrifugal force are indicated.

Figure 2 shows the vehicle geometrical parameters and the centre of mass (CoM) position of the whole system. It is assumed that the rider controls the longitudinal accelerations by properly acting on the front/rear bakes and throttle in order to produce the necessary longitudinal forces. Similarly, desired lateral accelerations are imposed by mean of the handlebar generating the suitable lateral forces. Consequently, longitudinal and lateral accelerations may be regarded as rider's controls.

The dynamic equations are obtained by means of the Newton-Euler approach, which yields the following six equations of motion:

$$
\begin{aligned}
&M a_x = S_r + S_f \\
&M a_y = F_r + F_f \\
&M g = N_r + N_f \\
&M a_y h \cos(\varphi) = M g h \sin(\varphi) \\
&M a_x h \cos(\varphi) = b\, N_r + (p-b) N_f \quad \text{sign is wrong} \\
&M a_x h \sin(\varphi) = b\, F_r + (p-b) F_f \quad \text{sign is wrong}
\end{aligned}
\tag{1}
$$

where $M$ is the mass, $p$ is the wheelbase, $b$, $h$ are the coordinates of the CoM, $a_x$ and $a_y$ are the longitudinal and lateral acceleration, $\varphi$ is the roll angle. $S$, $F$, $N$ are the longitudinal, lateral and vertical tire forces respectively, subscript $r$ is used for the rear tire while subscript $f$ is used for the front one.

$$
\alpha = \frac{S_r}{S_r + S_f} \tag{2}
$$

where $\alpha$ accounts for the percentage of total longitudinal force at the rear tire, therefore $\alpha = 1$ means longitudinal force only applied at the rear wheel. Based on the above assumptions, the motorcycle roll solely depends on the imposed lateral acceleration:

$$
\varphi = \arctan\left(a_y / g\right) \tag{3}
$$

whereas expressions of tire vertical forces show that the load transfer between the front and rear tire depends both on the longitudinal acceleration and on the lateral one due to the CoM height relationship with the roll angle:

$$
\begin{aligned}
N_r &= \left(a' + h' \cos\varphi\right) M g = \left(a' + h' \frac{a_x}{\sqrt{1 + a_y^2}}\right) M g \\
N_f &= \left(b' - h' \cos\varphi\right) M g = \left(b' - h' \frac{a_x}{\sqrt{1 + a_y^2}}\right) M g
\end{aligned}
\tag{4}
$$

where the non-dimensional CoM height $h' = h/p$ and longitudinal position $b' = b/p'$ $a' = (p-b)/p = 1 - b'$ have been introduced for convenience.

Finally, lateral and longitudinal tire forces are limited by tire adherence, which approximately is proportional to the tire load. In order to consider tire adherence constraints, it is convenient to refer to non-dimensional forces. The non-dimensional lateral forces have a very simple expression:

$$
\frac{F_r}{N_r} = \frac{F_f}{N_f} = \frac{a_y}{g} \tag{5}
$$

whereas the expressions of non-dimensional longitudinal forces are more complex:

$$
\frac{S_r}{N_r} = \frac{1}{a' + h' \frac{a_x}{\sqrt{1 + a_y^2}}} \frac{a_x}{g} \alpha \quad , \quad \frac{S_f}{N_f} = \frac{1}{b' - h' \frac{a_x}{\sqrt{1 + a_y^2}}} \frac{a_x}{g} (1 - \alpha) \tag{6}
$$

where $\alpha = 1$ in acceleration conditions ($a_x > 0$), while $0 < \alpha < 1$ in braking conditions ($a_x < 0$).

Since tire adherence is limited, *i.e.* tire forces must remain inside the friction ellipse, it is straightforward that not every set of given lateral and longitudinal accelerations are physically achievable. Assuming that tire adherence is proportional to the tire load and lateral and longitudinal forces as a function of imposed accelerations as in Equation

(5)-(6), adherence constraints for the rear and front tire are respectively:

$$\begin{aligned}&\left(\frac{S_r}{\mu_x N_r}\right)^2+\left(\frac{F_r}{\mu_y N_r}\right)^2=\left(\frac{f_{xr}}{\mu_x}\right)^2+\left(\frac{f_{yr}}{\mu_y}\right)^2=\left(\frac{1}{\mu_x}\frac{1}{a'+h'a_x\big/\sqrt{1+a_y^2}}\frac{a_x}{g}\alpha\right)^2+\left(\frac{1}{\mu_y}\frac{a_y}{g}\right)^2\leq 1\\&\left(\frac{S_f}{\mu_x N_f}\right)^2+\left(\frac{F_f}{\mu_y N_f}\right)^2=\left(\frac{f_{xf}}{\mu_x}\right)^2+\left(\frac{f_{yf}}{\mu_y}\right)^2=\left(\frac{1}{\mu_x}\frac{1}{b'-h'a_x\big/\sqrt{1+a_y^2}}\frac{a_x}{g}\left(1-\alpha\right)\right)^2+\left(\frac{1}{\mu_y}\frac{a_y}{g}\right)^2\leq 1\end{aligned}\tag{7}$$

where the tire engagement coefficient $f_x = S/N$ and $f_y = F/N$ have been introduce for further discussions. Those are the actual used forces normalized with the vertical load and are comparable with the adherence limits (*i.e.* how much the tire is used with respect to its limits). To proceed with the analysis, it is necessary to distinguish between traction and braking maneuvers.

**3.2 Combined Cornering and traction maneuvers**

When $a_x > 0$ a traction force is present only at the rear wheel ($\alpha = 1$) therefore the rear tire engagement is greater than the front one. Consequently, if the first inequality of (8) is satisfied, the second inequality is automatically satisfied too.

A second condition that must be avoided is the wheeling, *i.e.* the front tire load must remain positive. Moreover, the thrust force is limited by the available engine torque, but this aspect will be not discussed here. Summarizing, lateral and longitudinal acceleration are limited by the following two inequalities:

$$\begin{aligned}&\left(\frac{1}{a'+h'\dfrac{a_x}{\sqrt{1+a_y^2}}}\frac{a_x}{\mu_x g}\alpha\right)^2+\left(\frac{a_y}{\mu_y g}\right)^2\leq 1\\&N_f>0 \;\Rightarrow\; b'-h'\frac{a_x}{\sqrt{1+a_y^2}}>0\end{aligned}\tag{8}$$

which are represented in Figure 3 (a) upper part of the diagram. Figure shows that the maximum longitudinal accelerations are reached in combination with lateral ones (*i.e.* tilted motorcycle) and not in pure traction as expected. In fact the roll angle lowers the vehicle CoM reducing the load transfer between front and rear wheels, which is maximum for null roll angle as proved by Equation (4). Hence, the maximum traction performance are reached when the bike is exiting a curve, *i.e.* it is slightly tilted.

**3.3 Combined Cornering and braking maneuvers: front brake only**

When $a_x < 0$, a braking force is available both at the front and rear tires. Let us suppose here to use only the front brake at the maximum feasible value (later on the case of combined front and rear braking will be discussed). As a consequence, if the second inequality of (8) is satisfied, the first inequality is automatically satisfied too. In this case the additional condition to be avoided is the stoppie, *i.e.* the rear tire load must be positive. The inequalities that must be satisfied during braking maneuvers are the following:

$$\begin{aligned}&\left(\frac{1}{b'-h'a_x\big/\sqrt{1+a_y^2}}\frac{a_x}{\mu_x g}\right)^2+\left(\frac{a_y}{\mu_y g}\right)^2\leq 1\\&N_r>0 \;\Rightarrow\; a'+h'\frac{a_x}{\sqrt{1+a_y^2}}>0\end{aligned}\tag{9}$$

which can be represented along with Equations (8) in Figure 3 (a) (lower part of diagram). As for traction case, the maximum longitudinal deceleration is reached with the motorcycle slightly rolled due to a lower load transfer.

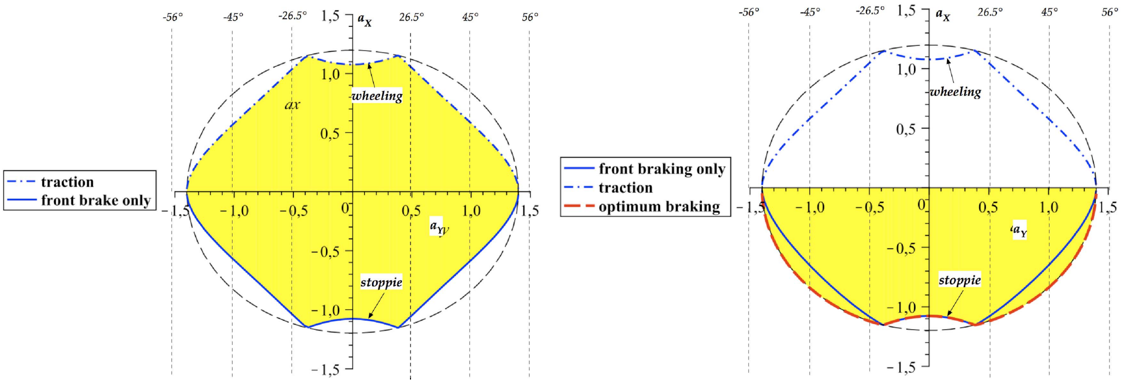


(a) Front brake only (b) Optimum braking strategy

Figure 3 – Theoretical g-g diagram for a motorcycle.

Two main considerations can be drawn from the theoretical g-g diagram. The first one is that, with roads of high friction coefficient (as in racing), the wheeling/stoppie conditions (*i.e.* inequalities) are the most restrictive. Those prevent the motorcycle to reach the maximum longitudinal de/accelerations in straight run. Secondly, a gain in longitudinal deceleration/acceleration is possible with tilted motorcycle due to a lower CoM and consequently a decrease in the load transfer. Finally, with combined lateral acceleration and longitudinal deceleration it is not possible to reach the tire adherence limit if only the front brake is used. Consequently the tire engagement is not maximize, and the acceleration envelope does not fill up the ellipse of adherence (yellow area in Figure 3 (a)). The first and second considerations point out the importance of vehicle design and the last one the rider's driving strategy, which will be discussed in the next two sections.

### 3.4 Optimal braking maneuvers

Let us remove the hypothesis of front brake only in order to calculate the optimal braking force repartition (*i.e.* parameter $\alpha$) and suppose that both front and rear tires experience the same engagement (work at maximum combined adherence limit) and that rear and front longitudinal ones are also the same:

$$\frac{f_{xf}^2}{\mu_x^2}+\frac{f_{yf}^2}{\mu_y^2}=\frac{f_{xr}^2}{\mu_x^2}+\frac{f_{yr}^2}{\mu_y^2} \quad , \quad f_{xf}=f_{xr} \tag{10}$$

Substituting Equation (3) to (6) in Equation (10) the optimal brake repartition and maximum acceleration is found as follows:

$$\alpha = 1-b+\sqrt{\frac{1}{a_y^2+1}}h\,a_x \quad , \quad a_x=\frac{\sqrt{\mu_Y^2-a_y^2}\,\mu_X}{\mu_Y} \tag{11}$$

Figure 3 (a) shows that the optimal braking maneuver (dash line), which uses also the rear brake, is able to reach the ellipse of adherence, except when stoppie condition occurs. There is a net gain in the maneuver performance which is quantified by the highlighted yellow area in the Figure. However, the optimal braking strategy acts to the tire limits and including the fact that the load torque of the engine in many cases is high enough to lock the rear wheel, only few racing riders are able to put into practice this optimum braking strategy. The same cannot be said for acceleration maneuvers since traction force is only available at the rear wheel.

### 3.5 Aerodynamic drag effect

Among the different simplification assumption, neglecting the aerodynamics drag is not realistic, especially for race motorcycle than can reach speed greater than 300 km/h. If the aerodynamic centre is not far to the vehicle CoM, only the first equation of (1) has to be modified as follows:

$$M\,a_x+\frac{1}{2}\rho C_D v^2=S_r+S_f \tag{12}$$

which introduces some complication into the discussion due to the dependence on the speed $v$. However, all considerations above remain valid in the sense that they give useful information about the combination of lateral and longitudinal forces that are compatible with tire adherence and other constraints, regardless the thrust force is needed to accelerate the vehicle or to overcame drag resistance.

## 4 How main motorcycle design parameters affect G-G diagrams

As shown above, the optimal braking strategy is rider's responsibility only, whereas the wheeling and stoppie conditions' detrimental effect may be reduced with a proper motorcycle design. Figure 4 (a) and (b) show the theoretical g-g diagrams for different position of the CoM (i.e. parameter $h'$ and $b'$). Diagram Figure 4 (a) shows that lower values of $h'$ reduce the load transfer in straight runs and allow for higher longitudinal accelerations. However, a net reduction of available longitudinal acceleration is obtained when lateral accelerations are presents. The effect is the same for braking conditions. However, here a good driver may fill the gap with a optimal braking strategy, which is not possible in traction. Moreover, further reduction will not bring advantages even in straight runs. On the other hand, rising the CoM will reduce the load transfer in straight runs but increase the acceleration performance in corners. This may be beneficial for motorcycle with low engine power that in any case prevent the vehicle to lift the front wheel in acceleration. The longitudinal position of the CoM has a different and opposite effect for braking and traction maneuvers as shown in Figure 4 (b).

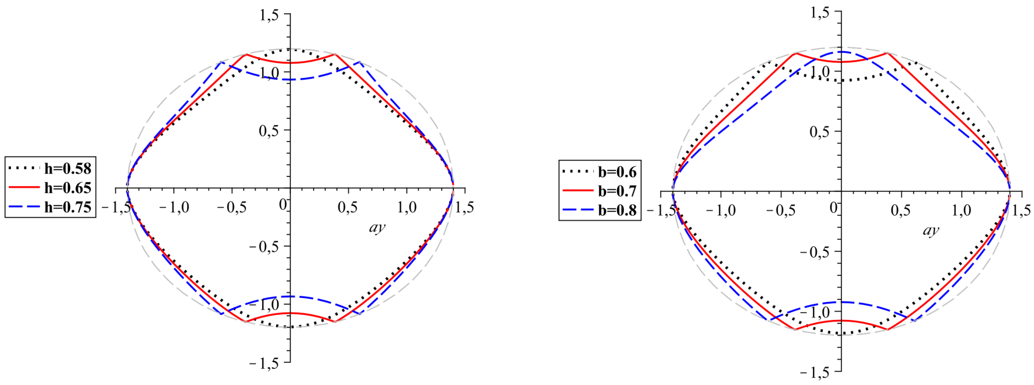


(a) CoM vertical position. $h'$ parameter (b) CoM horizontal position: $b'$ parameter

Figure 4 – Influence of CoM position.

## 5 Conclusions

The g-g diagrams produced by racing riders are a combination of motorcycle design choices and also driving strategy. Experimental evidence shows that racing riders are not able to completely fill the ellipse of adherence. In this work a theoretical explanation has been given with an interpretative model, which proved that the wheeling and stoppie conditions are the most limiting constrains for nearly straight runs, whereas rider's braking strategy is responsible for missing to fill the ellipse of adherence in braking maneuvers. Wheelie and stoppie constraint influence can be reduced with a proper design of the motorcycle.

## References

1 Milliken William, Douglas Milliken, "Race Car Vehicle Dynamics," SAE, ISBN 1-56091-526-9, 1995.
2 Rice, Roy, and Donald Alianello, "A Driver Characterizing Function, The g-g Diagram," Cornell Aeronautical Laboratory Report No.VJ-2882-K, June 1970.
3 Hisaoka Y., Yamamoto M., Okada A., "Closed-loop analysis of vehicle behavior during braking in a turn", JSAE Review, Vol. 20,No. 4, pp. 537-542, (1999)
4 Biral, F. Da Lio, M. Bertolazzi, E., "Combining safety margins and user preferences into a driving criterion for optimal control-based computation of reference maneuvers for an ADAS of the next generation", Proceedings, IEEE " Intelligent Vehicles Symposium 2005", 6-8 June 2005, pp 36- 41
5 Cossalter V., Da Lio M., Biral F., Fabbri L., "Evaluation of Motorcycle Manoeuvrability with the Optimal Manoeuvre Method", SAE Transanctions, Journal of Passenger Cars, 1998
6 Corno M., Savaresi S. M., Tanelli M., Fabbri L., " On optimal motorcycle braking", Control Engineering Practice, 16, pp. 644–657 , 2008.
7 Cossalter, V., Doria, A., Lot, R., "Optimum suspension design for motorcycle braking", Vehicle System Dynamics: International Journal of Vehicle Mechanics and Mobility, 34, 175–198, 2000.